Active load path adaption in a simple kinematic load-bearing structure due to stiffness change in the structure's supports

C M Gehb[1], R Platz[2] and T Melz[1]

[1] System Reliability and Machine Acoustics SzM, Technische Universität Darmstadt, Magdalenenstrasse 4, D - 64289 Darmstadt, Germany
[2] Fraunhofer Institute for Structural Durability and System Reliability LBF, Bartningstrasse 47, D - 64289 Darmstadt, Germany

E-mail: gehb@szm.tu-darmstadt.de

Abstract. Load-bearing structures with kinematic functions enable and disable degrees of freedom and are part of many mechanical engineering applications. The relative movement between a wheel and the body of a car or a landing gear and an aircraft fuselage are examples for load-bearing systems with defined kinematics. In most cases, the load is transmitted through a predetermined load path to the structural support interfaces. However, unexpected load peaks or varying health condition of the system's supports, which means for example varying damping and stiffness characteristics, may require an active adjustment of the load path. However, load paths transmitted through damaged or weakened supports can be the reason for reduced comfort or even failure. In this paper a simplified 2D two mass oscillator with two supports is used to numerically investigate the potential of controlled adaptive auxiliary kinematic guidance elements in a load-bearing structure to adapt the load path depending on the stiffness change, representing damage of the supports. The aim is to provide additional forces in the auxiliary kinematic guidance elements for two reasons. On the one hand, one of the two supports that may become weaker through stiffness change will be relieved from higher loading. On the other hand, tilting due to different compliance in the supports will be minimized. Therefore, shifting load between the supports during operation could be an effective option.

1. Introduction

Defined kinematics are often an important part of the functional performance in load-bearing systems with moving structural components. In most cases, the load is transmitted from one or more transmission points through a predetermined load path to the structural support interfaces. Examples are landing gear or suspension strut compression strokes in airplanes or vehicles. In these examples and on the one hand, a spring-damper system determines the main kinetic properties. On the other hand, the desired strokes are supported by kinematic elements like torque-links or other suspension links as an auxiliary structure that link two or more parts of a primer load structure for stability reasons. The load is distributed to the structural support interfaces as predetermined and, mostly, not subject to any change during the structure's lifetime. However, if properties or health conditions, e. g. damping and stiffness characteristics or strength of the supports vary over time, load path adaption, e. g. from a weaker support to a stronger one, could be an option to prevent the structure from failure or reduce comfort

Content from this work may be used under the terms of the Creative Commons Attribution 3.0 licence. Any further distribution of this work must maintain attribution to the author(s) and the title of the work, journal citation and DOI.
Published under licence by IOP Publishing Ltd

issues. Accordingly, it might be useful to change the load path and shift the load to the strongest support interfaces, e. g. with controlled adaptive auxiliary kinematic guidance elements capable to bear additional axial loading instead of passive torque-links or other suspension links.

To numerically investigate the potential of controlled active auxiliary kinematic guidance elements in a load-bearing structure, a simplified 2D two mass oscillator with two supports is used in this work. The adaptive functional extension of the active auxiliary kinematic guidance elements compared to passive torque-links or other suspension-links is to adapt the load path depending on the stiffness change of the supports.

An optimal design for the load path in a structural dynamic system like a truss with well known loading conditions and without moving structural components has been investigated thoroughly in literature, e. g. in [1] and [2]. In general, typical optimization parameters beside topology are cross section areas of truss members and the shape of trusses, [3]. Another approach for optimal truss design is possible via damage tolerance, [4]. In this approach, a simple 18-bar truss structure is designed to not collapse despite initial damage. These approaches improve the dynamic structural behavior and are based mainly on passive design without any external energy that is fed into the structure for adapting purposes. With additional energy fed into a structure, for example with actuators, a structure becomes active. However, the active approaches found in the literature mostly aim for an improvement in vibration control or damping. In [5] and [6], the authors used active joints with piezoelectric washers and stack actuators to improve the damping of two connected beams and a cantilever truss structure. The adaption or change of the load capacity was not investigated. Hence, studies to enhance the load capacity that could lead to load path adaption were made in [7] for a simple 9-bar truss with hydraulic jacks to apply internal forces and neuronal network as control strategy to react on unexpected high static load. In other studies, several beams of truss structures were substituted with idealized actuators in an academic way to enhance the load capacity by modifying the load path and to react to unknown loads, [8] and [9]. Both approaches used actuators in active beams which were able to change their axial length and, hence, the stiffness of the examined truss to create a fully stressed state of all the beams in the truss. In systems with movable structural components like landing gears or car-suspension, (semi-)active systems are used to enhance the dynamic of the system for vibration control, mostly controlled by the sky-hook control strategy [10], [11]. Load path adaption is again not addressed.

In this work, the simplified 2D two mass oscillator, assumed as a spring-damper-system between a lumped mass and a rigid beam supported by two support interfaces, is used to show the potential of load path adaption with active kinematic guidance elements numerically. Load path adaption might be necessary when one support becomes weaker due to damage or changes in the support's stiffness. Moreover, undesirable tilting leads to unbalanced positions. The basic idea is to shift loads that primarily go through the spring-damper also go through the kinematic guidance elements, [12]. Load path adaption will be possible if active forces are applied in the joints or hinges of the kinematic guidance elements that now become kinetic.

The simplified 2D two mass oscillator is derived from a complex load-bearing system that is currently developed in the German Collaborative Research Center (SFB) 805 "Control of Uncertainties in Load-Carrying Structures in Mechanical Engineering" at the Technische Universität Darmstadt. This load bearing system is called Modular Active Spring Damper System MASDS and is an example for a truss with integrated spring-damper system, figure 1(a).

Figure 1(a) shows the CAD model of the MASDS. The main parts are the upper and lower truss structure, a suspension strut from a mid-range car with a coil spring and a viscous damper as the spring-damper system, and kinematic guidance elements to realize a defined compression stroke between the upper and lower truss. The ratio of the masses of the upper and lower truss is similar to a typical quarter-car-model. The architecture of the whole MASDS is modular, for example it is possible to replace the passive suspension strut by an active spring-damper system,

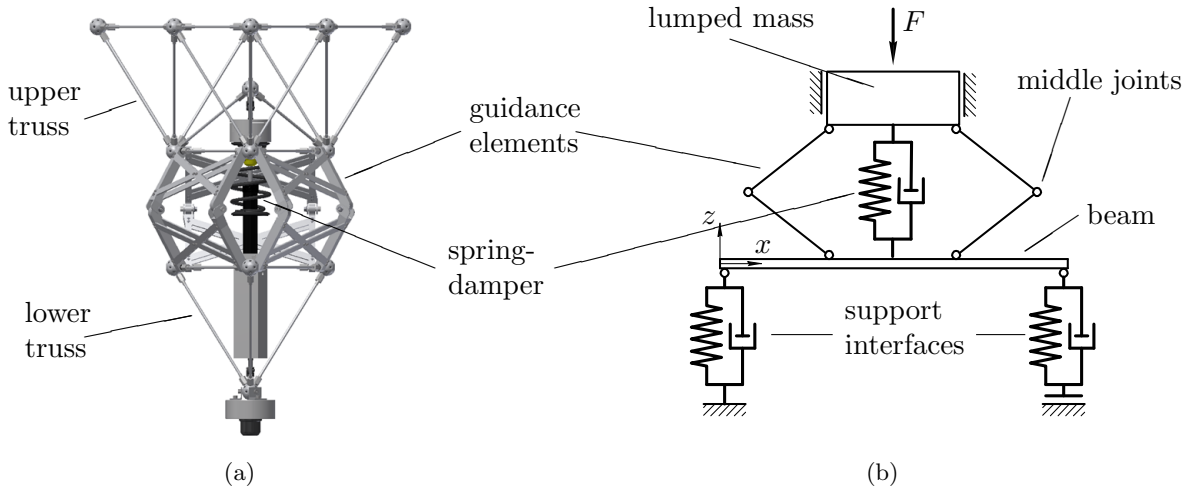

Figure 1. CAD Model of the MAFDS (a) and simplified 2D two mass oscillator (b)

[13].

For the following calculations, the 3D-structure of MASDS in figure 1(a) is simplified to a 2D two mass oscillator. Figure 1(b) shows the reduced two mass oscillating system with the guidance elements in 2D replacing the guidance elements in 3D. A lumped mass is connected to a rigid beam by a spring-damper-system and two guidance elements. The rigid beam is supported at its ends by support interfaces with varying damping and stiffness characteristics. The right support is assumed to be damaged by a reduced value of its stiffness parameter. The passive kinematic guidance elements will be replaced by active ones with active forces in the middle joints, section 2.

In case the kinematic guidance elements are passive, their main function is to enable the defined up-and-down compression stroke. They are not a part of the flux of forces between the two masses in z-direction in figure 1(b). With active guidance elements and the possibility to generate torques in the middle joints of the guidance elements a new load path can be generated, e. g. due to a disc brake or an electrodynamic actuator. In this case, the guidance elements are part of the flux of forces in z-direction.

In the following sections, the mathematical model of the two mass oscillator is derived and afterwards used for the numerical simulations. If both support's stiffnesses are the same, the rigid beam will not tilt. With decrease of stiffness in one support, however, the passive compressions are not balanced anymore and the beam tilts. Shifting the load away from the damaged support with less stiffness towards the undamaged support will be an option.

In a first step, the theoretical limits of compensable stiffness difference of the supports are calculated for the static case by the active guidance elements balancing the support's compression. In a second step the displacements and the reaction forces of the passive and active system's supports will be compared.

2. Mathematical Model of the simplified 2D-System

The dimensions and model parameter of the two mass oscillator system with three degrees of freedom are shown in figure 2(a). It has a lumped mass m_A and a rigid beam with the mass m_B with its moment of inertia Θ in x-z-plane and the associated vertical displacements in z_A and z_B co-ordinates and rotation in φ co-ordinate. The masses m_A and m_B are symmetrically connected by angular guidance elements ① and ② on each side of the beam at the contact points $x = a$ and $x = l - a$ and a suspension strut with a coil spring and a viscous damper with

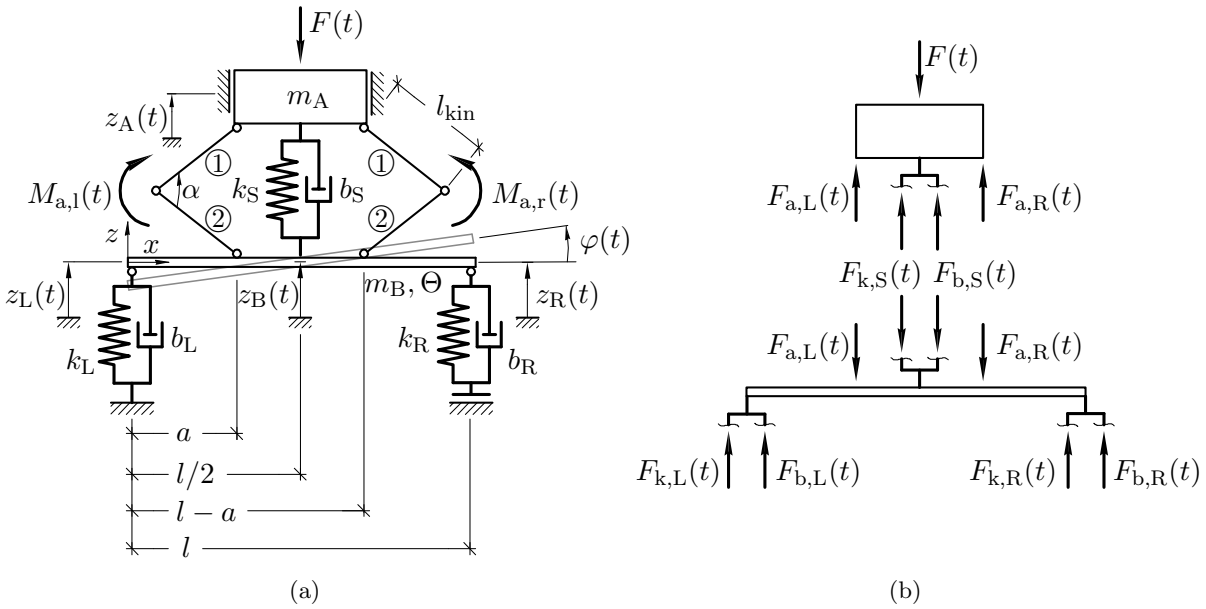

Figure 2. Simplified 2D two mass oscillator with active moments $M_{\mathrm{a,L}}(t)$ and $M_{\mathrm{a,R}}(t)$ in the kinematic guidance elements (a) and cut free forces (b)

stiffness k_{S} and damping coefficient b_{S} and at the middle of the beam $x = l/2$. The relative compression stroke is $z_{\mathrm{B}}(t) - z_{\mathrm{A}}(t)$. The beam is connected to the ground at $x = 0$ and $x = l$ by two supports represented by two springs and two dampers with stiffnesses k_{L} and k_{R} and damping coefficients b_{L} and b_{R} for left and right side. The suspension strut and the angular guidance elements are assumed to be free of mass. The linear displacements

$$z_{\mathrm{L}}(t) = \varphi(t)\,\frac{l}{2} - z_{\mathrm{B}}(t) \qquad \text{and} \qquad z_{\mathrm{R}}(t) = -\varphi(t)\,\frac{l}{2} - z_{\mathrm{B}}(t) \tag{1}$$

represent the compression of the supports for small angles $\varphi(t)$ with $\sin\varphi(t) \approx \varphi(t)$. The cut free spring force and damping force of the suspension strut are

$$F_{\mathrm{k,S}}(t) = k_{\mathrm{S}}\,[z_{\mathrm{B}}(t) - z_{\mathrm{A}}(t)], \tag{2a}$$
$$F_{\mathrm{b,S}}(t) = b_{\mathrm{S}}\,[\dot{z}_{\mathrm{B}}(t) - \dot{z}_{\mathrm{A}}(t)] \tag{2b}$$

and the cut free spring force and damping force of the supports are

$$F_{\mathrm{k,L}}(t) = k_{\mathrm{L}}\,z_{\mathrm{L}}(t) \qquad \text{and} \qquad F_{\mathrm{b,L}}(t) = b_{\mathrm{L}}\,\dot{z}_{\mathrm{L}}(t) \tag{3a}$$
$$F_{\mathrm{k,R}}(t) = k_{\mathrm{R}}\,z_{\mathrm{R}}(t) \qquad \text{and} \qquad F_{\mathrm{b,R}}(t) = b_{\mathrm{R}}\,\dot{z}_{\mathrm{R}}(t) \tag{3b}$$

with neglected forces in the x-direction. The combined support reaction forces and suspension strut force are

$$F_{\mathrm{L}}(t) = F_{\mathrm{k,L}}(t) + F_{\mathrm{b,L}}(t), \tag{4a}$$
$$F_{\mathrm{R}}(t) = F_{\mathrm{k,R}}(t) + F_{\mathrm{b,R}}(t), \tag{4b}$$
$$F_{\mathrm{S}}(t) = F_{\mathrm{k,S}}(t) + F_{\mathrm{b,S}}(t). \tag{4c}$$

The excitation force

$$F(t) = \begin{cases} 0 & \text{for } t < 0, \\ \widehat{F} & \text{for } t \geq 0. \end{cases} \tag{5}$$

is assumed as a step-function.

When considering a passive system without adaption of load path, the kinematic guidance elements have no kinetic use and additional forces and moments do not exist. When considering an active system with load path adaption, however, the kinematic guidance elements provide additional active moments $M_{\mathrm{a,L}}(t)$ and $M_{\mathrm{a,R}}(t)$, figure 2(a). $M_{\mathrm{a,L}}(t)$ and $M_{\mathrm{a,R}}(t)$ result in vertical active forces $F_{\mathrm{a,L}}(t)$ and $F_{\mathrm{a,R}}(t)$, figure 2(b), and are coupled by the kinematic transmission

$$M_{\mathrm{a,L}}(t) = l_{\mathrm{kin}} \cos\alpha \, F_{\mathrm{a,L}}(t), \tag{6a}$$

$$M_{\mathrm{a,R}}(t) = l_{\mathrm{kin}} \cos\alpha \, F_{\mathrm{a,R}}(t) \tag{6b}$$

with the length l_{kin} of each guidance component ① and ② and the relative angle α between ① and ②, figure 2(a).

A simple signal-based feedback PID-controller is implemented on the considered system. The input variable is the actual control deviation

$$e(t) = z_{\mathrm{L}}(t) - z_{\mathrm{R}}(t) \tag{7}$$

which is proportional to the support stiffness changes. Active control is assumed to be realized by actuators in the guidance elements. However, the actuator's dynamic behavior is neglected and it is assumed that the idealized actuators convert the controller output directly into the forces $F_{\mathrm{a,L}}$ and $F_{\mathrm{a,R}}$. Hence, the controller's output forces with $e(t)$ for the left and $\bar{e}(t) = -e(t)$ for the right guidance elements are

$$F_{\mathrm{a,L}}(t) = K_{\mathrm{P}}\, e(t) + K_{\mathrm{I}} \int e(t)\,\mathrm{d}t + K_{\mathrm{D}} \frac{\mathrm{d}\, e(t)}{\mathrm{d}t}, \tag{8a}$$

$$F_{\mathrm{a,R}}(t) = K_{\mathrm{P}}\, \bar{e}(t) + K_{\mathrm{I}} \int \bar{e}(t)\,\mathrm{d}t + K_{\mathrm{D}} \frac{\mathrm{d}\, \bar{e}(t)}{\mathrm{d}t}. \tag{8b}$$

In (8), K_{P} is the gain of the proportional component, K_{I} is the gain of the integral component and K_{D} is the gain of the derivation component. K_{P}, K_{I} and K_{D} are the tunable parameters of the PID-controller. They are determined by the Ziegler-Nichols tuning method and from that base fine-tuned empirically, [14].

According to the direction of cutting forces (2) and (3) in figure 2(b) the linear equation of motion for the upper mass m_{A} becomes

$$m_{\mathrm{A}} \ddot{z}_{\mathrm{A}}(t) + b_{\mathrm{S}}[\dot{z}_{\mathrm{A}}(t) - \dot{z}_{\mathrm{B}}(t)] + k_{\mathrm{S}}[z_{\mathrm{A}}(t) - z_{\mathrm{B}}(t)] = -F(t) + F_{\mathrm{a,L}}(t) + F_{\mathrm{a,R}}(t) \tag{9}$$

and for the beam m_{B}, Θ

$$\begin{aligned} &m_{\mathrm{B}} \ddot{z}_{\mathrm{B}}(t) + b_{\mathrm{S}}[\dot{z}_{\mathrm{B}}(t) - \dot{z}_{\mathrm{A}}(t)] + k_{\mathrm{S}}[z_{\mathrm{B}}(t) - z_{\mathrm{A}}(t)] - k_{\mathrm{L}}[\varphi(t)\,\frac{l}{2} - z_{\mathrm{B}}(t)] - b_{\mathrm{L}}[\dot{\varphi}(t)\,\frac{l}{2} \ldots \\ &-\dot{z}_{\mathrm{B}}(t)] - k_{\mathrm{R}}[-\varphi(t)\,\frac{l}{2} - z_{\mathrm{B}}(t)] + b_{\mathrm{R}}[\dot{\varphi}(t)\,\frac{l}{2} - \dot{z}_{\mathrm{B}}(t)] = -F_{\mathrm{a,L}}(t) - F_{\mathrm{a,R}}(t) \end{aligned} \tag{10a}$$

$$\begin{aligned} &\Theta\ddot{\varphi}(t) + k_{\mathrm{L}}\,\frac{l}{2}[\varphi(t)\,\frac{l}{2} - z_{\mathrm{B}}(t)] + b_{\mathrm{L}}\,\frac{l}{2}[\dot{\varphi}(t)\,\frac{l}{2} - \dot{z}_{\mathrm{B}}(t)] - k_{\mathrm{R}}\,\frac{l}{2}[-\varphi(t)\,\frac{l}{2} - z_{\mathrm{B}}(t)] \ldots \\ &\quad - b_{\mathrm{R}}\,\frac{l}{2}[\dot{\varphi}(t)\,\frac{l}{2} - \dot{z}_{\mathrm{B}}(t)] = (\frac{l}{2} - a)\,F_{\mathrm{a,L}}(t) - (\frac{l}{2} - a)\,F_{\mathrm{a,R}}(t) \end{aligned} \tag{10b}$$

for translational directions $z_{\mathrm{A}}(t)$ and $z_{\mathrm{B}}(t)$ as well as for rotational direction $\varphi(t)$, [15]. Equation (9) and (10) are combined to a linear equation of motion system to become

$$\underbrace{\begin{bmatrix} m_{\mathrm{A}} & 0 & 0 \\ 0 & m_{\mathrm{B}} & 0 \\ 0 & 0 & \Theta \end{bmatrix}}_{\boldsymbol{M}} \underbrace{\begin{bmatrix} \ddot{z}_{\mathrm{A}}(t) \\ \ddot{z}_{\mathrm{B}}(t) \\ \ddot{\varphi}(t) \end{bmatrix}}_{\ddot{\boldsymbol{r}}(t)} + \underbrace{\begin{bmatrix} b_{\mathrm{S}} & -b_{\mathrm{S}} & 0 \\ -b_{\mathrm{S}} & b_{\mathrm{S}}+b_{\mathrm{L}}+b_{\mathrm{R}} & -\frac{l}{2}\,b_{\mathrm{L}}+\frac{l}{2}\,b_{\mathrm{R}} \\ 0 & -\frac{l}{2}\,b_{\mathrm{L}}+\frac{l}{2}\,b_{\mathrm{R}} & \frac{l^2}{4}\,b_{\mathrm{L}}+\frac{l^2}{4}\,b_{\mathrm{R}} \end{bmatrix}}_{\boldsymbol{D}} \underbrace{\begin{bmatrix} \dot{z}_{\mathrm{A}}(t) \\ \dot{z}_{\mathrm{B}}(t) \\ \dot{\varphi}(t) \end{bmatrix}}_{\dot{\boldsymbol{r}}(t)} + \ldots$$

$$\underbrace{\begin{bmatrix} k_{\mathrm{S}} & -k_{\mathrm{S}} & 0 \\ -k_{\mathrm{S}} & k_{\mathrm{S}}+k_{\mathrm{L}}+k_{\mathrm{R}} & -\frac{l}{2}\,k_{\mathrm{L}}+\frac{l}{2}\,k_{\mathrm{R}} \\ 0 & -\frac{l}{2}\,k_{\mathrm{L}}+\frac{l}{2}\,k_{\mathrm{R}} & \frac{l^2}{4}\,k_{\mathrm{L}}+\frac{l^2}{4}\,k_{\mathrm{R}} \end{bmatrix}}_{\boldsymbol{K}} \underbrace{\begin{bmatrix} z_{\mathrm{A}}(t) \\ z_{\mathrm{B}}(t) \\ \varphi(t) \end{bmatrix}}_{\boldsymbol{r}(t)} = \underbrace{\begin{bmatrix} -F(t)+F_{\mathrm{a,L}}(t)+F_{\mathrm{a,R}}(t) \\ -F_{\mathrm{a,L}}(t)-F_{\mathrm{a,R}}(t) \\ (\frac{l}{2}-a)\,F_{\mathrm{a,L}}(t)-(\frac{l}{2}-a)\,F_{\mathrm{a,R}}(t) \end{bmatrix}}_{\boldsymbol{F}(t)}. \tag{11}$$

In (11), $\boldsymbol{M}$, $\boldsymbol{D}$ and $\boldsymbol{K}$ are the global mass, damping and stiffness matrices, $\ddot{\boldsymbol{r}}(t)$, $\dot{\boldsymbol{r}}(t)$, $\boldsymbol{r}(t)$ and $\boldsymbol{F}(t)$ are the acceleration, velocity, displacement and force vectors. The force vector $\boldsymbol{F}(t)$ in (11) contains the excitation force and the active forces $F_{\mathrm{a,L}}(t)$ and $F_{\mathrm{a,R}}(t)$ provided by the active guidance elements in figure 2(b).

The support's reaction forces $F_{\mathrm{L}}(t)$ and $F_{\mathrm{R}}(t)$ and displacements $z_{\mathrm{L}}(t)$ and $z_{\mathrm{R}}(t)$ of the supports at x=0 and x=l need to be calculated to investigate the ability to load path adaption, respectively re-direction. For that, it is necessary to solve (11) in time domain numerically. In state space representation, (11) becomes

$$\dot{\boldsymbol{x}}(t) = \underbrace{\begin{bmatrix} \mathbf{0} & \mathbf{I} \\ -\boldsymbol{M}^{-1}\,\boldsymbol{K} & -\boldsymbol{M}^{-1}\,\boldsymbol{D} \end{bmatrix}}_{[6\times 6]} \boldsymbol{x}(t) + \underbrace{\begin{bmatrix} \mathbf{0} \\ \boldsymbol{M}^{-1}\,\boldsymbol{B}_{\mathrm{a}} \end{bmatrix}}_{[6\times 2]} \boldsymbol{u}(t) + \underbrace{\begin{bmatrix} \mathbf{0} \\ \boldsymbol{M}^{-1}\,\boldsymbol{b}_{\mathrm{ext}} \end{bmatrix}}_{[6\times 1]} F(t)$$

$$\boldsymbol{y}(t) = \begin{bmatrix} 0 & -1 & \frac{l}{2} & 0 & 0 & 0 \\ 0 & 1 & \frac{l}{2} & 0 & 0 & 0 \\ 0 & -k_{\mathrm{L}} & \frac{l}{2}\,k_{\mathrm{L}} & 0 & -d_{\mathrm{L}} & \frac{l}{2}\,d_{\mathrm{L}} \\ 0 & k_{\mathrm{L}} & \frac{l}{2}\,k_{\mathrm{L}} & 0 & d_{\mathrm{L}} & \frac{l}{2}\,d_{\mathrm{L}} \end{bmatrix} \boldsymbol{x}(t) = \begin{bmatrix} z_{\mathrm{L}}(t) \\ z_{\mathrm{R}}(t) \\ F_{\mathrm{L}}(t) \\ F_{\mathrm{R}}(t) \end{bmatrix} \tag{12}$$

with the $[6 \times 1]$ state vector $\boldsymbol{x}(t) = [\boldsymbol{r}(t), \dot{\boldsymbol{r}}(t)]^T$ and zero and identity matrices $\mathbf{0}$ and $\mathbf{I}$ of appropriate dimensions. The active forces $F_{\mathrm{a,L}}(t)$ and $F_{\mathrm{a,R}}(t)$ and the external excitation force $F(t)$ are allocated to the system by the $[6 \times 2]$ control input matrix and the $[6 \times 1]$ excitation input vector

$$\boldsymbol{B}_{\mathrm{a}} = \begin{bmatrix} 0 & 0 \\ 0 & 0 \\ 0 & 0 \\ 1 & 1 \\ -1 & -1 \\ (\frac{l}{2}-a) & -(\frac{l}{2}-a) \end{bmatrix} \quad \text{and} \quad \boldsymbol{b}_{\mathrm{ext}} = \begin{bmatrix} 0 \\ 0 \\ 0 \\ 1 \\ 0 \\ 0 \end{bmatrix}. \tag{13}$$

The active forces are summarized in control input vector

$$\boldsymbol{u}(t) = \begin{bmatrix} F_{\mathrm{a,L}}(t) \\ F_{\mathrm{a,R}}(t) \end{bmatrix}. \tag{14}$$

In short form, (12) is

$$\begin{aligned} \dot{\boldsymbol{x}}(t) &= \boldsymbol{A}\,\boldsymbol{x}(t) + \boldsymbol{B}_{\mathrm{a}}\,\boldsymbol{u}(t) + \boldsymbol{b}_{\mathrm{ext}}\,F(t) \\ \boldsymbol{y}(t) &= \boldsymbol{C}\,\boldsymbol{x}(t) \end{aligned} \tag{15}$$

representing the state space model of the two mass oscillator with three degrees of freedom and active forces provided by the kinematic guidance elements. The time response of the reaction forces $F_{\mathrm{L}}(t)$ and $F_{\mathrm{R}}(t)$ and displacements $z_{\mathrm{L}}(t)$ and $z_{\mathrm{R}}(t)$ of the supports are chosen as output $\boldsymbol{y}(t)$, section 3. For deriving the dynamic equations for the two mass oscillator with controlled forces in its guidance elements, the right support is assumed to be damaged with reduced stiffness as described above. Because of this, only the left guidance element need to be active and with that $F_{\mathrm{a,R}}(t) \equiv 0$.

3. Numerical simulation of load path adaption

In this section, numerical simulations of the two mass oscillator are presented to prove its load path adaption capability. First, the theoretical limits of the compensable stiffness change for the static case is presented. Second, three cases for one example configuration with undamaged and damaged support are compared.

3.1. Theoretical limits of load path adaption in static case

The aim for the active kinematic guidance elements in the case of assumed stiffness change is to minimize the difference of the vertical support displacements $e(t) \stackrel{!}{=} 0$, cf. (7). Hence, full compensation of stiffness difference by means of the active guidance elements is achieved for $e(t) = 0$. However, a theoretical limit for the full compensation $e(t) = 0$ of stiffness change can be calculated for the time-independent static case. To satisfy $e = 0$ time-independent, the vertical support displacements have to be equal $z_{\mathrm{L}} = z_{\mathrm{R}}$. With that and all time derivations of the degrees of freedom take a value of zero, the combination of (1), (4) and (10) leads to

$$\frac{k_{\mathrm{L}}}{k_{\mathrm{R}}} = \frac{\dfrac{F_{\mathrm{a,L}}}{F_{\mathrm{S}}} + 1}{\dfrac{a}{l}\dfrac{F_{\mathrm{a,L}}}{F_{\mathrm{S}}} + \dfrac{1}{2}} - 1 \tag{16}$$

respectively

$$\kappa = \frac{\Lambda + 1}{\xi \cdot \Lambda + \dfrac{1}{2}} - 1. \tag{17}$$

To discuss the limit, the support stiffnesses difference is converted into the ratio of the stiffnesses $\kappa = k_{\mathrm{L}}/k_{\mathrm{R}}$, plotted on the vertical axis in figure 3. The ratio $\Lambda = F_{\mathrm{a,L}}/F_{\mathrm{S}}$ of the maximal assumed active force of the guidance element and the suspension strut force is given by the relation of $F_{\mathrm{a,L}}$ and F_{S}. The geometrical dimensions, particularly the contact points of the active guidance elements on the beam are taken into account by $\xi = a/l$.

All parameter combinations of κ, ξ and Λ leading to a point above the surface in figure 3, full compensation of the stiffness difference by means of active guidance elements is not possible, $e = z_{\mathrm{L}} - z_{\mathrm{R}} \neq 0$ meaning that load redistribution is not sufficient for full compensation. All parameter combinations of κ, ξ and Λ leading to a point on or under the surface in figure 3, full compensation of the stiffness difference is possible, $e = z_{\mathrm{L}} - z_{\mathrm{R}} = 0$.

No difference in stiffness is given for $\kappa = 1$ which represents the undamaged system. In this case no load path adaption is needed. The higher κ, the higher the stiffness difference of the supports. The lower ξ, the closer is the contact point to the support and the capability of load

path adaption increases. The higher Λ, the higher is the maximum active force $F_{\mathrm{a,L}}$ compared to the suspension strut force F_{S}. With higher Λ the capability of load path adaption increases. In the following, one example configuration was chosen to simulate a system with step-excitation in time domain.

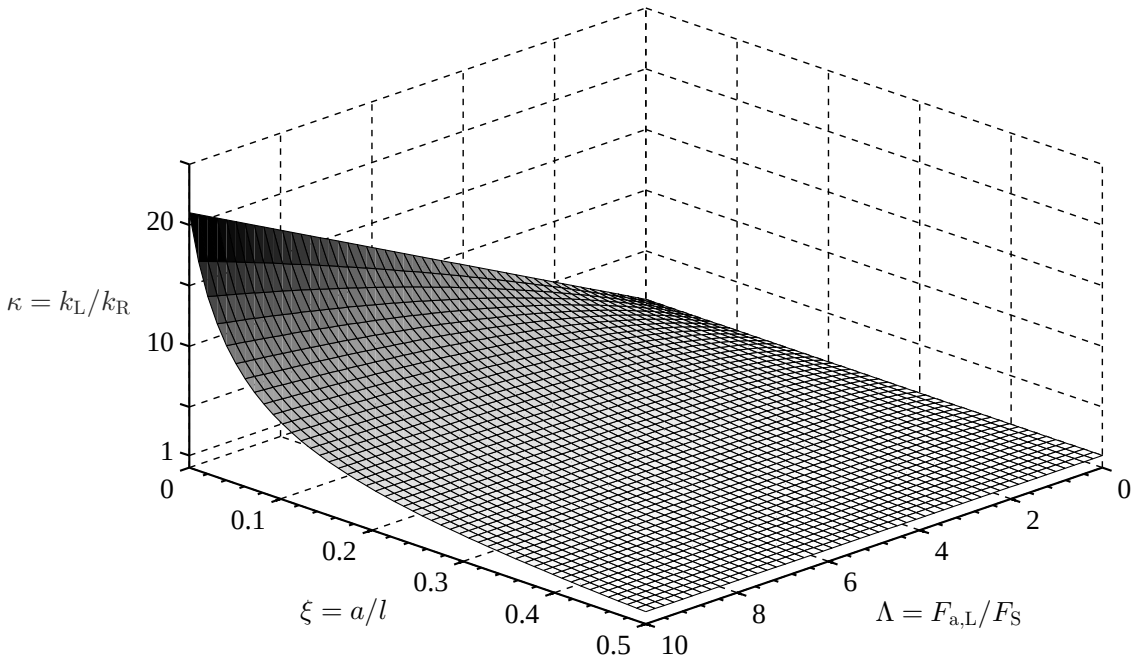

Figure 3. Limit of compensation of stiffness difference due to active load path adaption, for the area above the surface, compensation is not sufficient for $e = 0$

3.2. Step excitation and numerical results in time domain for an example configuration
The displacement difference $e(t) = z_{\mathrm{L}}(t) - z_{\mathrm{R}}(t)$ and the reaction forces $F_{\mathrm{L}}(t)$ and $F_{\mathrm{R}}(t)$ of the left and right support are shown in figures 4-7 as a result of a numerical simulation in time domain to prove the theoretic capability of the active force $F_{\mathrm{a,L}}(t)$ to shift load from the weaker support to the stronger one. Three different cases are investigated:

i) both supports have equal stiffnesses $\kappa = 1$, the system is passive and assumed to be without auxiliary kinetic function of the guidance elements,
ii) right support is assumed to be damaged with lower stiffness and $\kappa = 2$, the system is passive and assumed to be without auxiliary kinetic function of the guidance elements,
iii) right support is assumed to be damaged with lower stiffness and $\kappa = 2$, the system is active and assumed to be with auxiliary kinetic function of the guidance elements.

For all cases i)-iii), the step excitation (5) with $\widehat{F} = 1000$ N is applied to the system. Table 1 summarizes all properties of the two mass oscillator.

The displacement difference $e(t) = z_{\mathrm{L}}(t) - z_{\mathrm{R}}(t)$ according to the output $\boldsymbol{y}(t)$ in (15) for all three cases are shown in figure 4. In case i), the undamaged system without any stiffness difference, the displacement difference is $e(t) = z_{\mathrm{L}}(t) - z_{\mathrm{R}}(t) = 0$. Case ii) leads to a displacement difference $e(t) = z_{\mathrm{L}}(t) - z_{\mathrm{R}}(t) \neq 0$ for the whole simulation time $t = 0$ to 1.5 s and a constant steady state

Table 1. Parameters for 2D two mass oscillator with $\kappa = 2$ and $\xi = 0.25$.

property	symbol	value	unit
damping suspension	b_S	1100	Ns/m
stiffness suspension	k_S	27000	N/m
stiffness support left	k_L	500000	N/m
stiffness support right	k_R	500000	N/m
stiffness support right, damaged	k_R	250000	N/m
mass A	m_A	40	kg
mass B	m_B	200	kg
moment of inertia	Θ	16.7	$\mathrm{kg\,m^2}$
beam length	l	1	m
contact point	a	0.25	m
excitation step	$\widehat{F}$	1000	N

displacement difference for $t > 1\,\mathrm{s}$ after oscillations are damped out can be observed. In case iii) it seems possible to reduce the displacement difference after a transient oscillation again to $z_\mathrm{L}(t) - z_\mathrm{R}(t) = 0$ for $t > 1\,\mathrm{s}$ by means of active guidance elements.

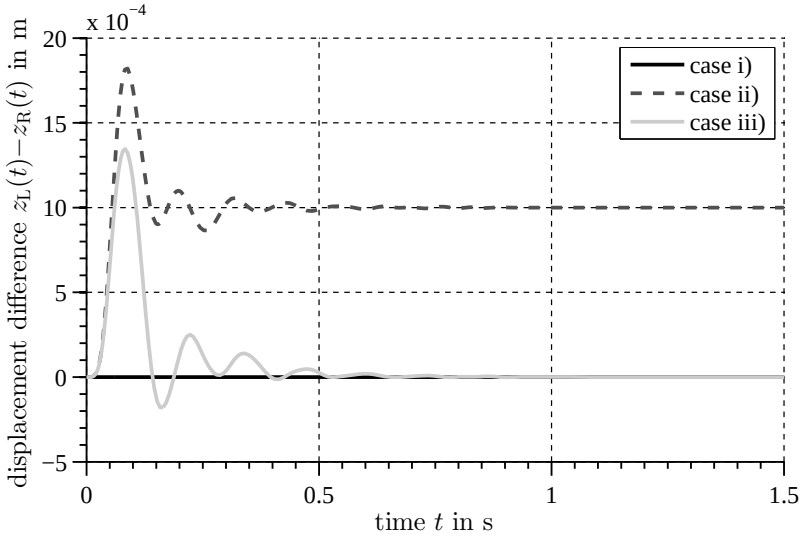

Figure 4. Numerical simulation of the displacement difference $z_\mathrm{L}(t) - z_\mathrm{R}(t)$ in the supports with $\kappa = 1\,\mathrm{to}\,2$ and $\xi = 0.25$

Figure 5 shows the support's reaction forces $F_\mathrm{L}(t)$ and $F_\mathrm{R}(t)$ for case i). The load is evenly distributed to both supports and the time responses of both reaction forces are similar. After the oscillations are damped out, the excitation load of $\widehat{F} = 1000\,\mathrm{N}$ is evenly split and both supports are loaded with 500 N. High Peak of 790 N is observed before the oscillations are damped.

Figure 6 shows the support's reaction forces $F_\mathrm{L}(t)$ and $F_\mathrm{R}(t)$ for case ii). The load is evenly distributed to both supports and the reaction forces are similar for $t > 1\,\mathrm{s}$ after oscillations are damped out. Peak forces in the left and right support are different. In the steady state $t > 1\,\mathrm{s}$, the excitation load of $\widehat{F} = 1000\,\mathrm{N}$ is again evenly split and both supports are loaded

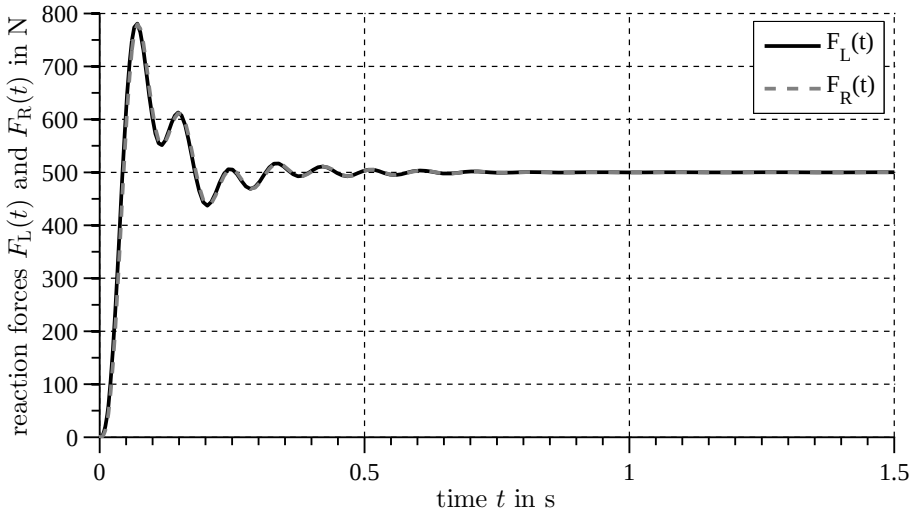

Figure 5. Numerical simulation of the reaction forces $F_{\mathrm{L}}(t)$ and $F_{\mathrm{R}}(t)$ in the supports for the undamaged system with $\kappa = 1$ and $\xi = 0.25$, case i)

with $F_{\mathrm{L}}(t) = F_{\mathrm{R}}(t) = 500\,\mathrm{N}$. Even though, the displacement difference of the supports is $e(t) = z_{\mathrm{L}}(t) - z_{\mathrm{R}}(t) \neq 0$, cf. figure 4. Beside the displacement difference, the oscillation phase regarding the load peaks of both supports is not equal any more as consequence of supports with different stiffnesses, $\kappa = 2$.

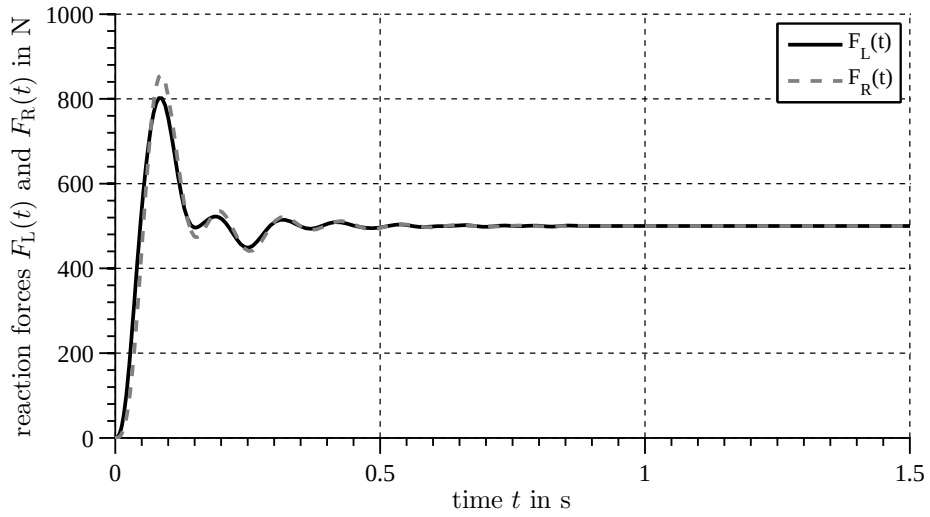

Figure 6. Numerical simulation of the reaction forces $F_{\mathrm{L}}(t)$ and $F_{\mathrm{R}}(t)$ in the supports for the damaged and passive system with $\kappa = 2$ and $\xi = 0.25$, case ii)

Figure 7 shows the support's reaction forces $F_{\mathrm{L}}(t)$, $F_{\mathrm{R}}(t)$ and the active force $F_{\mathrm{a,L}}(t)$ calculated by the controller in (8) for case iii). The load is not evenly distributed to both supports and the reaction forces $F_{\mathrm{L}}(t)$ and $F_{\mathrm{R}}(t)$ differ at all the times $0 \leq t \leq 1.5\,\mathrm{s}$, $F_{\mathrm{L}}(t) \neq F_{\mathrm{R}}(t)$. For $t \leq 1\,\mathrm{s}$, the excitation load $\widehat{F} = 1000\,\mathrm{N}$ is not evenly split and both supports are loaded differently corresponding to their stiffnesses. The displacement difference of the supports is

again $z_{\mathrm{L}}(t) - z_{\mathrm{R}}(t) = 0$ for $t > 1\,\mathrm{s}$, cf. figure 4. It can be seen that the active guidance elements are indeed changing the load path between the transmission point of the excitation force and the supports.

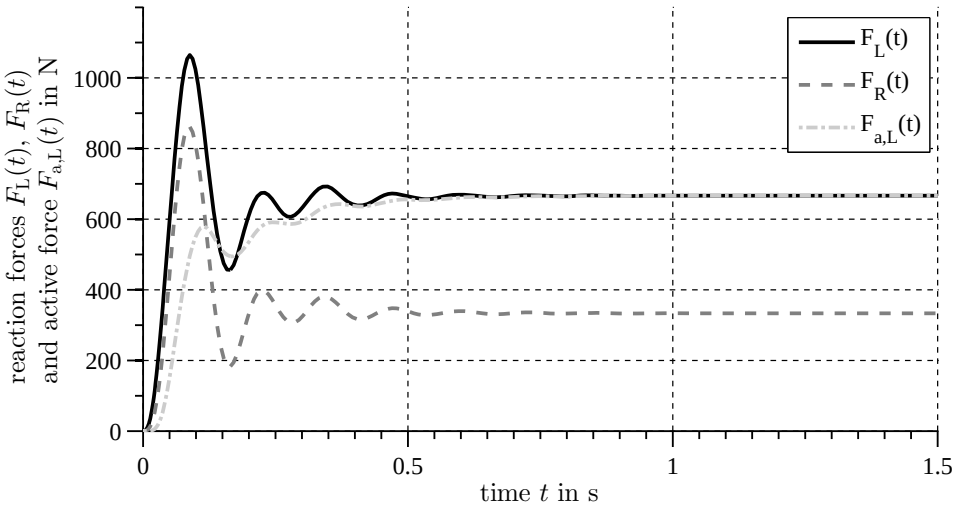

Figure 7. Numerical simulation of the reaction forces $F_{\mathrm{L}}(t)$ and $F_{\mathrm{R}}(t)$ in the supports for the damaged and active system with $\kappa = 2$ and $\xi = 0.25$, case iii)

4. Conclusions

This paper shows the potential of active auxiliary kinetic guidance elements in a simple two mass oscillator to adapt the load path with the guidance elements according to different stiffnesses of the supports by numerical simulation. The stiffness changes represent changing health condition of the elastic supports. Considering figures 4-7, it can be seen that active kinetic guidance elements has potential to provide an alternative load path in a load-bearing system and can be used to shift load from one support to another. In a first step the limits for a static load path adaption are shown depending on geometric and dynamic properties. The maximum difference of the stiffnesses that can be compensated depends on the geometric values and the active forces provided by the kinetic guidance elements. After that, in three cases the displacement difference and reaction forces of the two mass oscillator's supports are compared in numerical simulations in time domain with step excitation: in the first case, both supports are assumed to be undamaged with equal stiffnesses, the system remains passive without auxiliary kinetic function of the guidance elements. The load is evenly distributed to both supports, no active force is needed. In the second case, the right support is assumed to be damaged with reduced stiffness, the system remains passive without auxiliary kinetic function of the guidance elements. The stiffness difference leads to displacements difference of the supports if the load path is not controlled. In the third case, the right support is assumed to be damaged with reduced stiffness, the system is assumed to be active with auxiliary kinetic function of the guidance elements. The displacements difference of the supports and the tilt of the beam can be extinguished. This is possible by changing the load path by means of the active guidance elements. The damaged support is relieved. In future work, the model will be more detailed, e. g. the actuator behavior. Moreover, the results of this paper will be verified with experimental results.

Acknowledgments
The authors like to thank the German Research Foundation (DFG) for funding this project within the Collaborative Research Center (SFB) 805 "Control of Uncertainties in Load-Carrying Structures in Mechanical Engineering".

References

[1] Bendsøe M P, Ben-Tal A and Zowe J 1994 *Structural optimization* **7** 141–159
[2] Rajan S 1995 *Journal of Structural Engineering* **121** 1480–1487
[3] Farajpour I 2010 *Advances in Engineering Software* **41** 580–589
[4] Marhadi K S, Venkataraman S and Wong S A 2011 *Structural and Multidisciplinary Optimization* **44** 213–233
[5] Gaul L and Nitsche R 2000 *Zeitschrift für angewandte Mathematik und Mechanik* **80** 45–48
[6] Gaul L, Hurlebaus S, Wirnitzer J and Albrecht H 2008 *Acta Mechanica* **195** 249–261
[7] Joghataie A 2001 *Neural Network World* **11** 285–292
[8] Lemaitre C 2008 *Topologieoptimierung von adaptiven Stabwerken* Ph.D. thesis University Stuttgart Dept. Civil and Environmental Engineering
[9] Teuffel P 2004 *Entwerfen adaptiver Strukturen - Lastpfadmanagement zur Optimierung tragender Leichtbaustrukturen* Ph.D. thesis University Stuttgart Dept. Civil and Environmental Engineering
[10] Unger A F 2012 *Serientaugliche quadratisch optimale Regelung für semiaktive Pkw-Fahrwerke (engl. Series-ready quadratic optimal control for semi-active passenger car chassis)* Ph.D. thesis Technische Universität München
[11] Do A L, Spelta C, Savaresi S and Sename O 2010 *IEEE Conference on Decision and Control* **49** 5560–5565
[12] Gehb C M, Platz R and Melz T 2015 *Proc. SPIE 9433, Industrial and Commercial Applications of Smart Structures Technologies 2015* vol 9433 (San Diego, USA) pp 94330G–94330G–9 URL `http://dx.doi.org/10.1117/12.2086491`
[13] Bedarff T, Hedrich P and Pelz P 2014 (*Proc. 9. IFK* vol 3)
[14] Visioli A 2006 *Practical PID Control* (Springer)
[15] Markert R 2013 *Strukturdynamik (engl. Structural Dynamics)* (Shaker Verlag)